

Journal of Materials Chemistry A

Accepted Manuscript



This is an *Accepted Manuscript*, which has been through the Royal Society of Chemistry peer review process and has been accepted for publication.

Accepted Manuscripts are published online shortly after acceptance, before technical editing, formatting and proof reading. Using this free service, authors can make their results available to the community, in citable form, before we publish the edited article. We will replace this *Accepted Manuscript* with the edited and formatted *Advance Article* as soon as it is available.

You can find more information about *Accepted Manuscripts* in the [Information for Authors](#).

Please note that technical editing may introduce minor changes to the text and/or graphics, which may alter content. The journal's standard [Terms & Conditions](#) and the [Ethical guidelines](#) still apply. In no event shall the Royal Society of Chemistry be held responsible for any errors or omissions in this *Accepted Manuscript* or any consequences arising from the use of any information it contains.

Elastic Ionogels with Freeze-aligned Pores Exhibit Enhanced Electrochemical Performances as Anisotropic Electrolytes of All-solid-state Supercapacitors

Received 00th January 20xx,
Accepted 00th January 20xx

DOI: 10.1039/x0xx00000x

Xinhua Liu^a, Baofeng Wang^{*b}, Zilu Jin^a, Huanlei Wang^c and Qigang Wang^{*a}

www.rsc.org/

Bio-inspired by the bone materials, the hierarchical porous materials with aligned structure have been designed and applied in various fields. However, the realization of anisotropic function based on the aligned structure is still a challenge. Herein, we prepare nanocomposite ionogel electrolytes with aligned porous structures via a directional freezing of BMIMPF₆, PEGMA (PEGDA), and TiO₂ at -18 °C and further TiO₂-initiated cryopolymerization under UV-irradiation. The crystal of PEG derivatives at -18 °C provides a directional template for the formation of aligned porous structures within the ionogel networks. The additional TiO₂ nanoparticles, as photoinitiators and nanofillers, endow the aligned ionogels with high mechanical strength. The aligned ionogel-based supercapacitor exhibits anisotropic electrochemical performances and flexibility. The specific capacitance of the device with the vertically aligned ionogel is 172 F g⁻¹ at the current density of 1 A g⁻¹, which is larger than the parallel aligned and non-aligned device.

Bio-inspired by the naturally aligned bone materials, aligned micrometre-sized porous materials have shown significant importance in biomedical engineering,¹ electronics,²⁻⁴ and energy storage devices.⁵⁻¹⁰ Whereas, ionic conducting polymer gels with aligned structures have promising applications in modern electronics and multidisciplinary fields due to their accelerated ionic transports in large pores, semi-solid state and flexibility compared to some inorganic solid electrolytes.¹¹⁻¹⁵ Conventional polymer electrolytes prepared by the physical mixing and in-situ polymerization methods can be used in flexible and portable electric devices, such as electro-active actuators,¹⁶⁻¹⁸ supercapacitors,¹⁹⁻²² lithium batteries,²³ dye sensitized solar cells²⁴ and fuel cells.²⁵ However, they can hardly balance the confliction between maintaining necessary mechanical strength and electrochemical properties due to the lack of

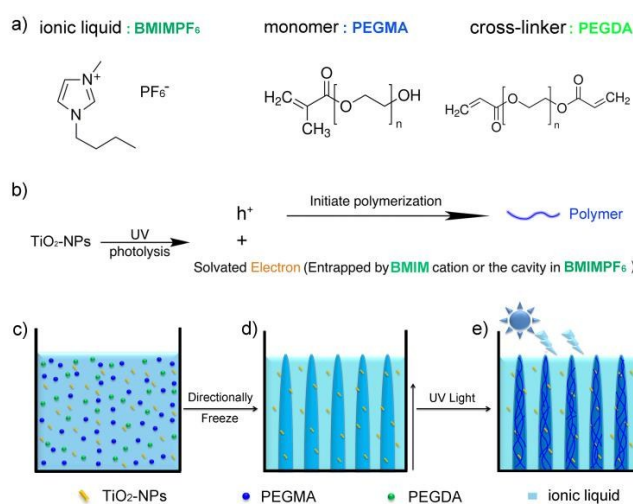


Fig.1 Proposed mechanism of the crosslinked aligned ionogel from a monomer precursor solution. (a) The molecular structures. (b) The mechanism of the TiO₂-NPs initiated UV polymerization. (c) The precursor solution. (d) The ionic liquid molecules are excluded during directionally freezing between the orientated monomer crystals. (e) The monomers are polymerized in the frozen state to produce an aligned structure.

hierarchical structure within the gel matrix. An aligned porous structure within ionogels can endow them the similar ionic conductivity with pure ionic liquid in vertical direction, combined with the obvious enhanced thermal stability and mechanical strength.²⁶

Ice-templating process is a simple yet versatile method to facilitate the preparation of extensive hierarchical porous materials.^{27,28} Generally, a solution (or colloidal suspension) is to freeze in cold liquid and then produce the porous structures after freeze-drying to remove solvent.^{29,30} Cooper's group introduced a directional freezing approach of employing building blocks (polymers, nanoparticles or their mixtures) to prepare aligned porous materials. This approach was claimed to be able to achieve both good mechanical properties and desired hierarchically porous structure perfectly.³¹ As a pioneering example, Tomsia's group employed an ice-templating method and a low-temperature

^a Department of Chemistry and Advanced Research Institute, Tongji University, Shanghai 200092 (P. R. China). wangqg66@tongji.edu.cn

^b College of Environmental and Chemical Engineering, Shanghai University of Electric Power, Shanghai, 200090 (P. R. China). wangbaofeng@shiep.edu.cn

^c Institute of Materials Science and Engineering, Ocean University of China, Qingdao 266100 (P. R. China).

† Electronic Supplementary Information (ESI) available: The detailed experimental procedures, sample pre-treatments and various characterizations are provided.

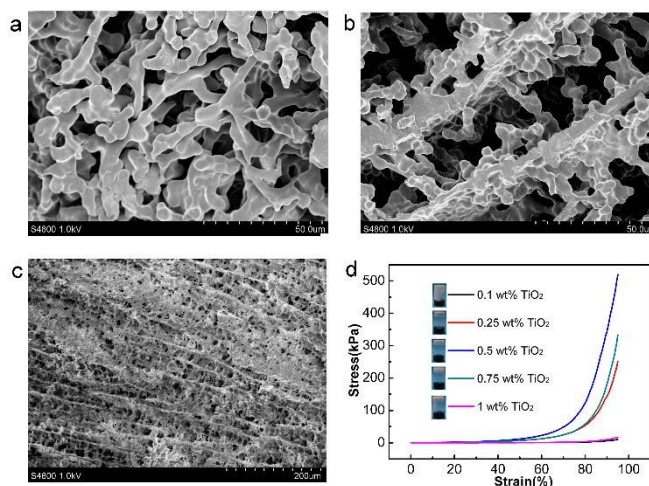


Fig.2 SEM images of the three-dimensional composites after vacuum freeze-drying. (a) non-aligned porous structure; (b,c) aligned porous structures; (d) Compressive curves of the ionogels with different TiO_2 contents via cryopolymerization.

polymerization to prepare a thermo-responsive composite hydrogels with hierarchical structures.³² Up to now, this approach is rarely applied in the preparation of ionogel with high mechanical strength.

Herein, we designed a simple directional templating ionogels with aligned porous structures. The aligned ionogels are appropriate electrolytes in flexible supercapacitors because of their excellent electrochemical behaviours from the aligned structures. The aligned ionogel electrolytes have the following components: 1-N-butyl-3-methylimidazolium hexafluorophosphate (BMIMPF_6), TiO_2 nanoparticles (TiO_2 -NPs), and poly (ethylene glycol) methacrylate (PEGMA, $M_n=500$) consisting of 5 wt% poly (ethylene glycol) dimethacrylate (PEGDA, $M_n=700$) (shown in Fig. 1a). The PEGMA and PEGDA were taken as the crystal temple considering their high melting points at about 25 °C.³³ Ionic liquids, BMIMPF_6 , 1-butyl-3-methylimidazolium bis[(trifluoromethyl) sulfonyl]imide (BMIMTFSI), and 1-butyl-3-methyl imidazolium tetrafluoroborate (BMIMBF_4) were selected because of their different melting points and excellent electrochemical properties. TiO_2 nanoparticles were used as the photoinitiator for the polymerization of monomers and as a reinforced nanofiller to enhance the mechanical strength of the ionogel via the supramolecular effect.³⁴⁻³⁶

As an example, 0.005 g TiO_2 -NPs and 0.100 g PEGMA (PEGDA) were dissolved in 0.895 g BMIMPF_6 via magnetic stirring for 30 min to form a viscous solution (Fig. 1c). Hole (h^+) and electron can be generated from the TiO_2 -NPs under UV irradiation (Fig. 1b) after which the electron can be entrapped either by BMIM^+ or the cavity in ionic liquid to form solvated electron and the hole can serve as the initiator to react with the monomers.^{18,36} Furthermore, the radicals of the chain growth can be validated by electron paramagnetic resonance (EPR) spectrum through UV irradiation (Fig. S1, ESI†). The gelation kinetics were further confirmed by using the time sweep measurements for monitoring the crossover points between the storage modulus (G') and the loss modulus (G'') (Fig. S2, ESI†). The frequency sweep curves illustrate substantial gel-like elastic

responses ($G' > G''$) of the ionogels with various TiO_2 contents (Fig. S3, ESI†). In this case, the final conversion of the monomers was over 93% after 2.5 hours of UV irradiation (Fig. S4, ESI†).

Finally, an aligned ionogel (aligned) can be obtained through UV cryopolymerization of the solid precursor for 2.5 hours at a temperature of -18 °C (Fig. 1e). The cold UV-light (with an average intensity of 99.8 mW/cm^2 at 365 nm) was selected in the cryopolymerization process to avoid any possible thermal impacts. Fig. S5, ESI† shows the changes of G' and G'' of the aligned ionogels as a function of the angular frequency, which also indicate a gel-like elastic performance.

The scanning electron microscope (SEM) images in Fig. 2a-2c demonstrate the porous structures of the ionogels. The vertically aligned structures presented in the cryopolymerized ionogels while being frozen directionally. As a control experiment, the polymerized samples without directional freezing cannot form an aligned structure. The PEG-based monomers can be directionally frozen in a reactor maintained at a temperature of about -18 °C (in Fig. S6, ESI†). The aligned structures in Fig. 2b and 2c can be attributed to the directional crystals of monomers.

As shown in Fig. 2d and S7, the ionogels display good mechanical strength in compressive tests and elastic response in loading-unloading curves. Compared to conventional initiators, the TiO_2 -NPs with an average size of 25 nm (Fig. S8) can also act as the inorganic cross-linking point for cryopolymerization of ionogels without any leakage of the ionic liquid (Fig. S9).³⁴⁻³⁶ When TiO_2 -NPs increased from 0.25 wt% to 0.5 wt%, the Young's modulus increased from 1.6 kPa to 21.2 kPa. The ionic conductivities of the ionogels with different TiO_2 contents have no great difference. The optimum amount of TiO_2 -NPs is 0.5 wt%. The ionogel with specific aligned porous structures (aligned) is able to keep a similar high mechanical strength (Fig. S10, ESI†) relative to the non-aligned porous ionogel (non-aligned). At last, these elastic ionogels are both designed as electrolytes for all solid-state supercapacitors.

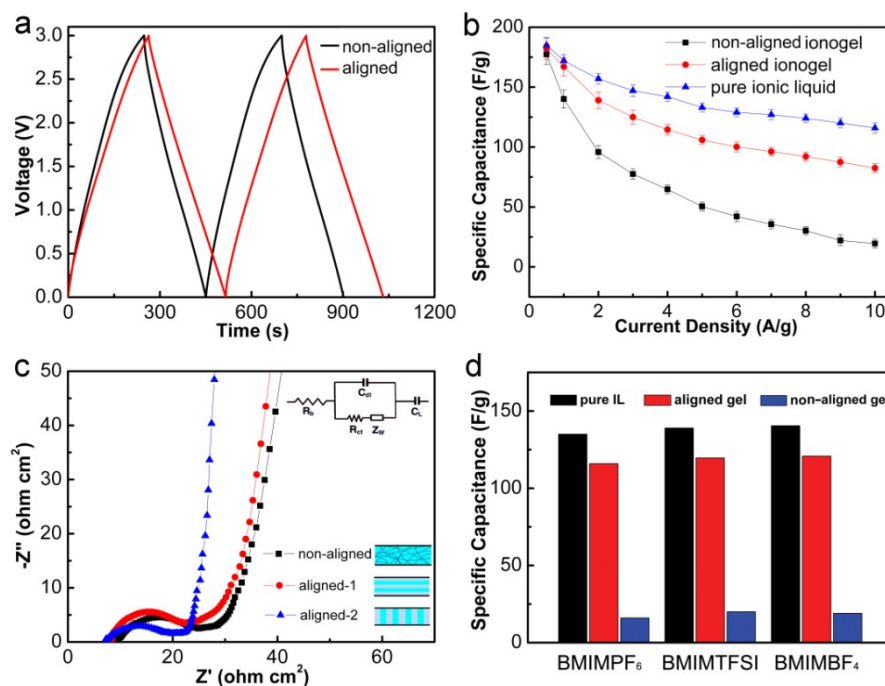


Fig.3 Electrochemical properties. (a) Galvanostatic charge-discharge curves of the ionogel electrolyte based supercapacitors measured at 1 A/g. (b) The correlation of specific capacitance with various current densities. (c) The impedance plots of supercapacitors with different ionogel structures at room temperature. (d) The specific capacitances of supercapacitors with different electrolytes at $-18\text{ }^{\circ}\text{C}$.

Herein, carbon nanocages (CNC700) with a specific surface area of $1810\text{ m}^2\text{ g}^{-1}$ were selected as supercapacitor electrode materials.³⁷ The SEM, TEM, nitrogen sorption isotherms, and the pore size distributions are shown in Fig. S11 and S12 (ESI[†]). Two carbon nanocage electrodes and an ionogel film were sandwiched in all solid state supercapacitor. The calculated ionic conductivity of the non-aligned ionogel was 1.06 mS/cm (Fig. S13, ESI[†]). In contrast, the ionogel with aligned structures provided a value of 1.46 mS/cm , which is close to the pure BMIMPF₆ (1.57 mS/cm).³⁸ The aligned ionogel-based supercapacitor exhibits a more rectangular cyclic voltammogram curve than the non-aligned one (Fig. S14, ESI[†]), which implies the enhanced electrochemical performance of the aligned device.

The charge and discharge curves are shown in Fig. 3a, which can be seen as the indication of capacitive performances. The aligned ionogel based supercapacitor achieved a high specific capacitances (C_{sp}) value of 172 F/g at the current density of 1 A/g , while the value of the non-aligned device was only 140 F/g . The aligned supercapacitor possesses fast charging and discharging behaviors (Fig. S15, ESI[†]). It is obvious that the aligned ionogel-based device performed better in maintaining higher C_{sp} values at higher current densities than the non-aligned one (Fig. 3b). Notably, the electrochemical performance of the ionogel with regularly aligned structures is comparable to the pure ionic liquid electrolyte-based device, thus further advocating the use of the aligned structures in electrochemical applications. Fig. S16 and S17 (ESI[†]) also can indicate the enhanced performance for aligned ionogel devices with BMIMTFSI and BMIMBF₄.

The enhanced electrochemical properties of the aligned ionogel can be attributed to easier ion transferring between electrode/electrolyte

interfaces and quicker ionic mobility within gel electrolyte. The different pore distribution of the aligned and non-aligned ionogels measured by the Hg intrusion (Fig. 4) can be employed as the explanation of the enhanced performance. The network of aligned ionogel exhibits a 68.7% porosity by utilizing ethanol to go into the pores and regular pores at $1\text{-}2$ and $8\text{-}10$ micrometers by mercury intrusion measurement. As the control, the network of non-aligned ionogel has only 42.4% of porosity and wild pores distribution from $0.01\text{-}10$ micrometers. The aligned ionogel with more effective big pores can host more free ions thus can accelerate the ion transfer across the electrode/electrolyte interfaces and ion mobility within electrolyte. However, the lower porosity and the existing of capillary pores within non-aligned ionogel have a worse ion movement across the interfaces and within gel matrix.

As shown in Fig. 3c, the impedance spectra has an arc at the higher frequency area and a spike at the lower frequency area. The impedance plots of supercapacitors with different ionogel structures suggests the lower bulk resistance of the vertical aligned ionogel based supercapacitor. The bulk resistances mainly attributed to the ionogel electrolytes exhibit that $R_{b\text{-aligned-}2} < R_{b\text{-aligned-}1} \approx R_{b\text{-non-aligned}}$. The different semicircles in the high frequency range correspond to the charge transfer resistance (R_{ct}) caused by the double layer capacitance on the surface. The Warburg resistance (Z_w) is the result of the frequency dependent ion transport. C_L is the limit capacitance. The results indicate that only the vertical direction can benefit the ions transports within ionogel matrix and on the surface of the electrode materials. The resistances of the ionogels increase proportionally with the increased thickness, while the resistivities have no relation to with the thicknesses of the ionogels (Fig. S13, ESI[†]).

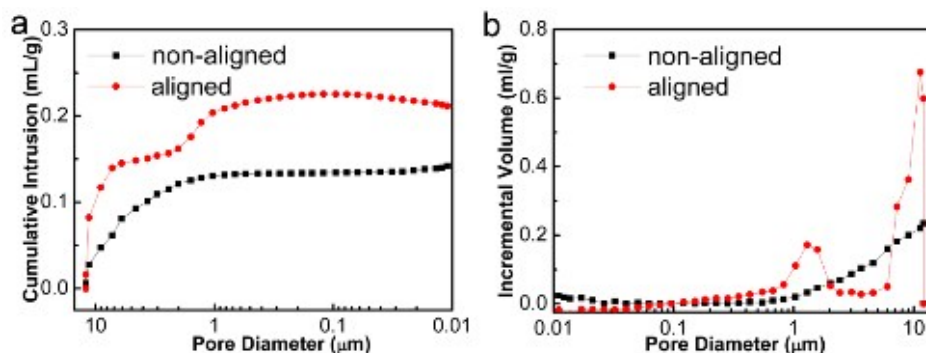


Fig.4 Pore distribution of the aligned and non-aligned ionogels. (a) Hg cumulative intrusion, and (b) Hg incremental volume versus pore diameter of the aligned and non-aligned samples.

Amazingly is that the resistivity is anisotropic in the aligned ionogel. The vertical direction (aligned-2) and parallel directions (aligned-1) have $6.9 \Omega \text{ m}$ and $9.1 \Omega \text{ m}$ resistivity, respectively. The aligned-1 ionogel has the similar resistivity to the non-aligned one ($9.3 \Omega \text{ m}$) due to the parallel pores, which could not provide effective ion pathways. The differences in ion pathways and resulting ionic mobility within various types of ionogels can be described in the Equation S1 and Fig. S18, ESI†. To validate this assumption, the electrochemical properties of the ionogel with parallel aligned structures were measured. The parallel ionogel exhibits a similar ionic conductivity (1.02 mS/cm) and an equivalent specific capacitance (139 F/g at the current density of 1 A/g) to the non-aligned ionogel for the fabrication of supercapacitor. The results further illustrate the electrochemical enhancements of the vertically aligned ionogel based devices.

The aligned-ionogel based supercapacitor possesses excellent capacitive performance at a wide temperature range from $-18 \text{ }^\circ\text{C}$ to $200 \text{ }^\circ\text{C}$ (Fig. S19, ESI†). The pure ionic liquids, aligned ionogels, and non-aligned ionogels of these ionic liquids were used as electrolytes for supercapacitors at low temperature ($-18 \text{ }^\circ\text{C}$). Fig. 3d represents that the aligned-ionogel-supercapacitors can maintain high Csp retention rates of 85%, 86% and 85% of the devices with corresponding pure ionic liquids at 0.05 A/g . However, the non-aligned devices had the lowest specific capacitance values. This easy ion transport near the porous electrode proves our previous hypothesis that the monomers are the real crystal temple for the aligned process. As shown in Fig. S20, the ionic liquids fail to crystallize during the cooling process.³⁹ In order to further verify this assumption, the precursor was then frozen in liquid nitrogen via the same cryopolymerization. The obtained aligned ionogel based device also illustrated similar electrochemical performances (Fig. S21, ESI†). Further, the aligned ionogel based device demonstrated a good stability (Fig. S22, ESI†). Additionally, our flexible supercapacitors exhibited excellent mechanical and electrochemical robustness in various bending tests (Fig. S23, ESI†), indicating the potential of the flexible supercapacitors in practice.

In conclusion, ionogels with aligned porous structures are prepared by directionally freezing method and further cryopolymerization, which possess significant improvement in electrochemical properties comparing to non-aligned one. It is expected that the proposed

method is able to provide a guidance to prepare aligned ionic conducting ionogels combining the advantages of mechanical strength and electrochemical functions. The elastic ionogels with aligned pores have great potentials to be the integrated electrolytes and separators for the facile fabrication of various flexible energy devices.

Acknowledgements

This work was supported by the National Science Foundation of China (No.21274111), the Program for New Century Excellent Talents in University of Ministry of Education of China (NECT-11-0386), the Fundamental Research Funds for Central Universities, and the Recruitment Program of Global Experts.

Notes and References

- 1 E. Salnikov, M. Rosay, S. Pawsey, O. Ouari, P. Tordo and B. Bechinger, *J. Am. Chem. Soc.*, 2010, **132**, 5940.
- 2 A. Yamaguchi, F. Uejo, T. Yoda, T. Uchida, Y. Tanamura, T. Yamashita and N. Teramae, *Nat. Mater.*, 2004, **3**, 337.
- 3 A. Walcarius, E. Sibottier, M. Etienne and J. Ghanbaja, *Nat. Mater.*, 2007, **6**, 602.
- 4 H. Gu, R. Zheng, X. Zhang and B. Xu, *Adv. Mater.*, 2004, **16**, 1356.
- 5 T. Chen, L. Qiu, H. G. Kia, Z. Yang and H. Peng, *Adv. Mater.*, 2012, **24**, 4623.
- 6 T. Chen, Z. Cai, L. Qiu, H. Li, J. Ren, H. Lin, Z. Yang, X. Sun and H. Peng, *J. Mater. Chem. A*, 2013, **1**, 2211.
- 7 T. Chen, L. Qiu, Z. Cai, F. Gong, Z. Yang, Z. Wang and H. Peng, *Nano lett.*, 2012, **12**, 2568.
- 8 H. Wang, D. Kong, P. Johanes, J. J. Cha, G. Zheng, K. Yan, N. Liu and Y. Cui, *Nano lett.*, 2013, **13**, 3426.
- 9 W. Weng, H. Lin, X. Chen, J. Ren, Z. Zhang, L. Qiu, G. Guan and H. Peng, *J. Mater. Chem. A*, 2014, **2**, 9306.
- 10 H. Lin, W. Weng, J. Ren, L. Qiu, Z. Zhang, P. Chen, X. Chen, J. Deng, Y. Wang and H. Peng, *Adv. Mater.*, 2014, **26**, 1217.
- 11 M. L. Hammock, A. Chortos, B. C. K. Tee, J. B. H. Tok and Z. Bao, *Adv. Mater.*, 2013, **25**, 5997.
- 12 Z. Yang, J. Deng, X. Chen, J. Ren and H. Peng, *Angew. Chem. Int. Ed.*, 2013, **52**, 13453.

- 13 P. Docampo, J. M. Ball, M. Darwich, G. E. Eperon and H. J. Snaith, *Nat. Commun.*, 2013, **4**, 2761 doi: 10.1038/ncomms3761.
- 14 T. Tamura and H. Kawakami, *Nano lett.*, 2010, **10**, 1324.
- 15 H. Xia, H. L. Wang, W. Xiao, M. O. Lai, and L. Lu, *Int. J. Surface Science and Engineering*, 2009, **3**, 23.
- 16 K. Mukai, K. Asaka, K. Kiyohara, T. Sugino, I. Takeuchi, T. Fukushima and T. Aida, *Electrochim Acta*, 2008, **53**, 5555.
- 17 B. He, Z. Wang, M. Li, K. Wang, R. Shen and S. Hu, *IEEE-ASME T Mech*, 2014, **19**, 312.
- 18 X. Liu, B. He, Z. Wang, H. Tang, T. Su and Q. Wang, *Sci. Rep.*, 2014, **4**, 6673; DOI:10.1038/srep06673.
- 19 K. Jost, D. Stenger, C. R. Perez, J. K. McDonough, K. Lian, Y. Gogotsi and G. Dion, *Energ Environ Sci*, 2013, **6**, 2698.
- 20 X. Liu, D. Wu, H. Wang and Q. Wang, *Adv. Mater.*, 2014, **26**, 4370.
- 21 X. Liu, D. Wu, H. Wang, J. Yang and Q. Wang, *J. Mater. Chem. A*, 2014, **2**, 11569.
- 22 X. Liu, P. Shang, Y. Zhang, X. Wang, Z. Fan, B. Wang and Y. Zheng, *J. Mater. Chem. A*, 2014, **2**, 15273.
- 23 J.-H. Shin, W. A. Henderson and S. Passerini, *J. Electrochem. Soc.*, 2005, **152**, A978.
- 24 D. Qin, Y. Zhang, S. Huang, Y. Luo, D. Li and Q. Meng, *Electrochim Acta*, 2011, **56**, 8680.
- 25 B. Lin, L. Qiu, J. Lu and F. Yan, *Chem. Mater.* 2010, **22**, 6718.
- 26 J. Le Bideau, L. Viau and A. Vioux, *Chem. Soc. Rev.*, 2011, **40**, 907.
- 27 M. C. Gutiérrez, M. L. Ferrer and F. del Monte, *Chem. Mater.*, 2008, **20**, 634.
- 28 L. Qian and H. Zhang, *Journal of chemical technology and biotechnology*, 2011, **86**, 172.
- 29 J. Zhu, J. Wang, Q. Liu, Y. Liu, L. Wang, C. He and H. Wang, *J. Mater. Chem. B*, 2013, **1**, 978.
- 30 M. Barrow, A. Eltmimi, A. Ahmed, P. Myers and H. Zhang, *J. Mater. Chem.*, 2012, **22**, 11615.
- 31 H. Zhang, I. Hussain, M. Brust, M. F. Butler, S. P. Rannard and A. I. Cooper, *Nat. Mater.*, 2005, **4**, 787.
- 32 H. Bai, A. Polini, B. Delattre and A. P. Tomsia, *Chem. Mater.*, 2013, **25**, 4551.
- 33 C. V. Nicholas, D. J. Wilson, C. Booth and J. R. Giles, *British polymer journal*, 1988, **20**, 289.
- 34 S. Dong, B. Zheng, D. Xu, X. Yan, M. Zhang and F. Huang, *Adv. Mater.*, 2012, **24**, 3191.
- 35 G. Yu, X. Yan, C. Han and F. Huang, *Chem. Soc. Rev.*, 2013, **42**, 6697.
- 36 D. Zhang, J. Yang, S. Bao, Q. Wu and Q. Wang, *Sci. Rep.*, 2013, **3**, 1399 doi:10.1038/srep01399.
- 37 K. Xie, X. Qin, X. Wang, Y. Wang, H. Tao, Q. Wu, L. Yang and Z. Hu, *Adv. Mater.*, 2012, **24**, 347.
- 38 W. Li, Z. Zhang, B. Han, S. Hu, Y. Xie and G. Yang, *J. Phys. Chem. B*, 2007, **111**, 6452.
- 39 A. R. Choudhury, N. Winterton, A. Steiner, A. I. Cooper and K. A. Johnson, *J. Am. Chem. Soc.*, 2005, **127**, 16792.

Table of Content

The directional-freezing construction of tough ionogel electrolytes with integrated functions through self-initiated UV cryopolymerization is described, which offers an effective approach for ionogel electrolytes to attain aligned structures and resulting enhanced electrochemical properties for energy storage devices.

